# Conceptual and Experimental Tools to Understand Spatial Effects and Transport Phenomena in Nonlinear Biochemical Networks Illustrated with Patchy Switching

Rebecca R. Pompano,[1] Andrew H. Chiang,[2] Christian J. Kastrup,[3] and Rustem F. Ismagilov[4]

[1]Department of Chemistry, University of Virginia, Charlottesville, Virginia 22904; email: rrp2z@virginia.edu

[2]Department of Chemistry and Institute for Biophysical Dynamics, The University of Chicago, Chicago, Illinois 60637; email: achiang@uchicago.edu

[3]Michael Smith Laboratories and Department of Biochemistry and Molecular Biology, University of British Columbia, Vancouver, British Columbia V6T 1Z4, Canada; email: ckastrup@mail.ubc.ca

[4]Division of Chemistry and Chemical Engineering, California Institute of Technology, Pasadena, California 91125; email: rustem.admin@caltech.edu

Annu. Rev. Biochem. 2017. 86:333–56

The *Annual Review of Biochemistry* is online at biochem.annualreviews.org

https://doi.org/10.1146/annurev-biochem-060815-014207



## Keywords

state switching, signaling, flow, mass transfer, Damköhler number, microfluidics

## Abstract

Many biochemical systems are spatially heterogeneous and exhibit nonlinear behaviors, such as state switching in response to small changes in the local concentration of diffusible molecules. Systems as varied as blood clotting, intracellular calcium signaling, and tissue inflammation are all heavily influenced by the balance of rates of reaction and mass transport phenomena including flow and diffusion. Transport of signaling molecules is also affected by geometry and chemoselective confinement via matrix binding. In this review, we use a phenomenon referred to as patchy switching to illustrate the interplay of nonlinearities, transport phenomena, and spatial effects. Patchy switching describes a change in the state of a network when the local concentration of a diffusible molecule surpasses a critical threshold. Using patchy switching as an example, we describe conceptual tools from nonlinear dynamics and chemical engineering that make testable predictions and provide a unifying description of the myriad possible experimental observations. We describe experimental microfluidic and biochemical tools emerging to test conceptual predictions by controlling transport phenomena and spatial distribution of diffusible signals, and we highlight the unmet need for in vivo tools.

## Contents



# INTRODUCTION

Biochemical reactions rarely occur in a perfectly homogeneous environment. With the exception of a well-mixed test tube, molecules and cells are dispersed unevenly through complex matrices, whether inside a cell, culture dish, or tissue. Furthermore, the reactions themselves are moving in space—molecules and cells are transported by diffusion, convection, and cellular motion, except when bound to relatively stationary support structures such as the extracellular matrix (ECM).

Historically, scientists have had better tools for controlling rates of reactions than for manipulating transport phenomena. Quantification of the rates of reactions affecting signaling molecules—for example, rate of enzymatic activity, rate of cellular secretion, and levels of gene expression—is standard in biological experiments, and modulating reaction rates (via small molecules, siRNA, inactivating antibodies, etc.) is common in basic science and medicine. In contrast, characterization and especially control of transport phenomena (1)—for example, diffusion, flow, effects of spatial arrangement, and effects of binding to the ECM (2–4)—have been more challenging. Yet, when these experiments are performed, they suggest that changes in transport rates can be significant enough to perturb the local concentration of a signal. For example, binding of basic fibroblast growth factor (bFGF) to heparan sulfate ($K_d \sim 24$ nM) slows its diffusion (5) through the basement membrane by >125-fold. Such a large change in local concentration can strongly affect the state of a biochemical network when the kinetics of the network depend nonlinearly on concentration (6). If a system shows threshold dependence on the concentration of the signal [e.g., in growth factor signaling (7)], this change may be sufficient to drive switching to a new state.

# TRANSPORT AND THRESHOLD KINETICS DRIVE PATCHY SWITCHING

## Definition of Patchy Switching

To illustrate the interplay of nonlinear reaction kinetics, changes in local concentrations, and mass transport phenomena, in this review we focus our attention on biological systems that switch their

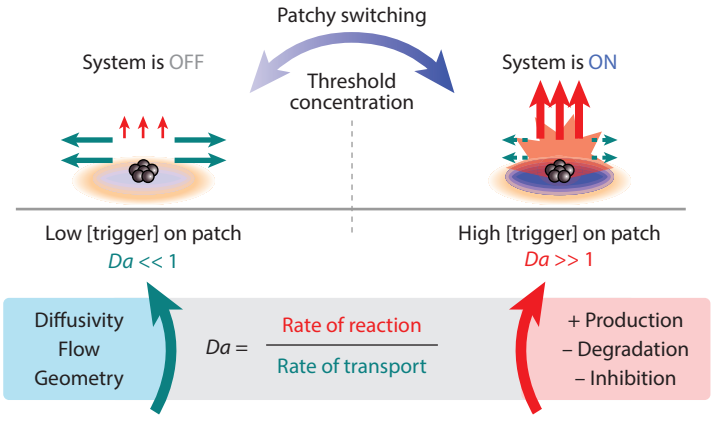


**Figure 1**

In patchy switching, local accumulation of diffusible triggers causes transitions between biological states, shown here for OFF and ON (*red starburst*) states. Triggers accumulate to high concentration (*dark blue*) only when their removal by transport (*green arrows*) is slower than their net production (*red arrows*). The competition between reaction and transport is described by a unitless quantity termed the Damköhler number (*Da*).

state in response to a change in local concentrations of diffusible molecules, which we call triggers (**Figure 1**). Although this phenomenon may sound specialized, it is actually quite common. Intuitive examples of state switching occur in blood coagulation (clotted/not clotted), cellular signaling networks (signaling on/off), quorum sensing (swarming/resting), neural dynamics (firing/not firing), and stem cell differentiation (pluripotent/differentiated). For a more rigorous description of state switching, we refer the reader to reviews of dynamical systems (8) and transitions between macro states in statistical thermodynamics (9). Triggers that control the state of a system as a result of a change in concentration include small molecules, proteins, and enzymes. For simplicity, here we focus on molecular triggers, although such state switching may also occur in response to changes in the local concentration of larger structures, such as vesicles or cells. All of these molecular triggers are subject to mass transport, and therefore their local concentrations are controlled by the balance of production, degradation, and mass transport phenomena.

A dramatic effect arises if two conditions are met: (*a*) triggers are localized or produced in a cluster we call a patch and (*b*) the system can switch from OFF to ON when triggers are present above a critical threshold concentration. When the local concentration of triggers near a patch passes through its critical threshold value, we call the state change patchy switching (**Figure 1**). For a concrete example, consider a small injury to a blood vessel that exposes blood to a patch of subendothelial tissue. This patch of damaged vasculature contains proteins, including tissue factor (TF) and collagen, which begin adhering platelets and activating an enzymatic cascade that can lead to a blood clot (10). Clotting occurs only when activated enzymes accumulate above a threshold concentration (11, 12), so this scenario meets the two conditions described above. Whether or not a clot forms and grows from the patch of damage depends on the balance between the net rate of enzyme activation (activation minus consumption and inhibition) and the rate of removal of those enzymes by flow or diffusion (13).

The concept of patchy switching is not new, though appreciation for it has remained mostly confined to specific fields. Switching driven by mass transport effects is predicted by classical theory in chemistry, including work by Turing on the chemical basis of morphogenesis and work

on the chemical dynamics of nonequilibrium systems (14, 15), and related approaches in chemical engineering (16). Patchy switching phenomena are a core concept in mathematical biology and ecology, especially in the context of population dynamics (17, 18). The critical balance among production, rapid degradation, and limited transport of growth factors through the extracellular matrices is a factor in tissue engineering design (3, 19); this balance has also been described for cancer niches and microenvironments (20, 21) and stem cell signaling (22). In this review, we use these ideas to illustrate the underlying principles that can describe many seemingly disparate examples of switching from biochemistry and cell and tissue biology.

Although any nonlinear system will respond to any change in spatial distribution (23), we have chosen to focus on the specific example of patchy switching because conceptually it is relatively simple, yet it can show dynamics that appear counterintuitive unless transport phenomena are considered. Now is an exciting time to study the effects of spatial distribution and mass transport of diffusible signals because newly emerging microfluidic and biochemical tools are revealing the interplay of reactions, transport, and spatial effects on the cellular scale. Throughout this review, we speculate on biochemical systems in which phenomena such as patchy switching are likely to occur, and we provide suggestions on how emerging tools might be used to probe these systems.



## Dynamics of Patchy Switching Predicted by the Damköhler Number

The relationship between transport and concentration in dynamical systems can quickly become complex, making it difficult to model and develop the intuition to make predictions. For example, in blood coagulation, the transport of coagulation enzymes is influenced by diffusion, flow, binding to cell surfaces and protein scaffolds, and secretion from platelets; importantly, the reaction network displays nonlinear responses due to multiple positive and negative feedback reactions. How does one begin to interpret and probe the interplay of reactions and transport phenomena in complex systems like this? Fortunately, concepts from chemical engineering can be used to unify the seemingly disparate features of a system, such as reaction rate, clustering of molecules, and binding to the ECM, into a single coherent description. For example, for patchy switching, all of these features are integrated into a simple dimensionless number that predicts the state of the system, termed the Damköhler number (*Da*). *Da* is the ratio of production and transport, and conveniently it can be defined in terms of either rates ($R$, 1/s or mol/s) or timescales ($\tau$, s):

$$Da = \frac{R_{\text{reaction}}}{R_{\text{removal}}} = \frac{\tau_{\text{removal}}}{\tau_{\text{reaction}}}$$

When $Da \gg 1$, triggers exceed a threshold concentration and the system will turn ON, whereas when $Da \ll 1$ the system will turn OFF (**Figure 1**). It is important to note that these are net rates. Thus, $R_{\text{reaction}}$ is the net rate of the production of triggers—in other words, it is equal to the difference between the total rate of all reactions that produce triggers and the total rate of all reactions that degrade or inhibit them. Alternatively, using timescales enables the estimation of *Da* even when rates are unknown. Thus, $\tau_{\text{reaction}}$ can be defined empirically as the time needed for a system to reach the threshold concentration of the trigger (in the absence of transport). Similarly, $R_{\text{removal}}$ and $\tau_{\text{removal}}$ refer to the net removal of triggers from the region of the patch by mass transport phenomena: diffusion, flow, transport by motile cells, etc. For example, in a system in which triggers are produced by the patch, $\tau_{\text{removal}}$ would be decreased by faster flow past the patch, whereas it would be increased by the trigger binding to matrix structures. Changes in spatial distribution drive patchy switching by changing $\tau_{\text{removal}}$.

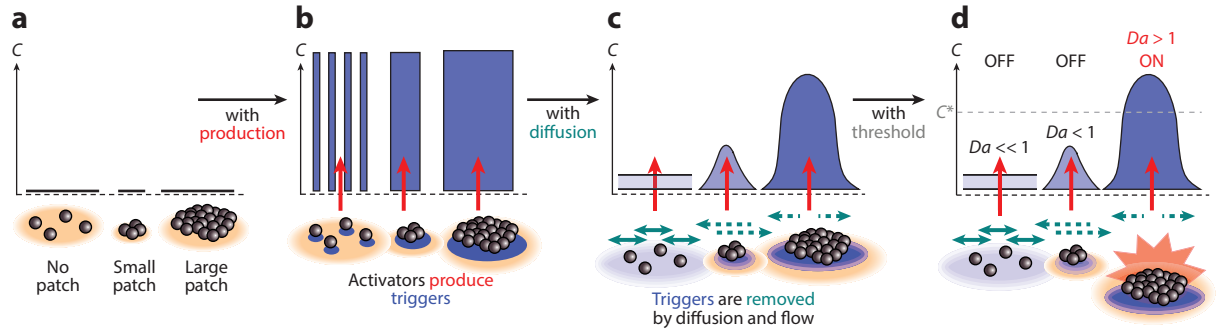


**Figure 2**

Balance of production and removal of triggers controls patchy switching and is described by the Damköhler number (*Da*). In each panel, the plot above depicts the concentration of triggers (*C*) for each scenario. (*a*) Three scenarios for the distribution of activators (*gray spheres*). "No patch" refers to molecules or cells being dispersed. (*b*) Activators produce triggers (*blue*) at a fixed rate per activator (*red arrows*). (*c*) Diffusion removes triggers (*green arrows*) with greater effect on smaller patches. (*d*) For a certain threshold concentration of triggers ($C^*$, *gray dotted line*), only the large patch accumulates triggers above the threshold and has $Da > 1$ (ON, *red starburst*). The no patch and small patch groups are both below the threshold and have $Da < 1$ (OFF).

## Predicting Patchy Switching in Response to Patch Size

As one example of the effect of spatial distribution on the state of a nonlinear biological system, consider the effect of patch size. Suppose that a patch consists of a cluster of activators (e.g., TF molecules). Each activator produces triggers (e.g., activated clotting enzymes) at a constant rate. Therefore, $\tau_{\text{reaction}}$ is independent of the size of the patch in the absence of mass transport. Thus, isolated activators, small patches, and large patches all would increase the local concentration of the trigger on the same timescale (**Figure 2*a*,*b***). In contrast, $\tau_{\text{removal}}$ depends on the size of the patch. For diffusion, the timescale is $\tau_D \sim x^2/D$ (seconds), where $x$ is the radius of the patch (meters) and $D$ is the diffusion constant ($m^2/s$) of the trigger. A freely diffusing trigger is removed rapidly from isolated molecules or cells, more slowly from a small patch, and slowest from a large patch (**Figure 2*c***). Removal of a trigger by flow would have a pattern similar to diffusion but is not depicted here. In summary, the larger the patch, the more the trigger accumulates. For a sufficiently large patch (larger than a so-called critical patch size), *Da* is $\gg 1$, and the trigger accumulates above the threshold concentration to turn the system ON (e.g., clotted). In contrast, systems with smaller or no patches remain OFF ($Da \ll 1$) (**Figure 2*d***). Thus, changes in the size of a patch can also initiate patchy switching. Once state switching is initiated, it can even propagate outward from the patch (e.g., **Figure 3*a***) in the presence of positive feedback loops, such as autocatalytic production of thrombin during blood clotting (24).

We emphasize that this example of state switching is not meant to be all-encompassing. We use this type of patchy switching (switching ON when the local concentration of diffusible molecules crosses a threshold) throughout the review for clarity, but the tools and methods described apply to a broad range of state switching systems in which mass transport phenomena play a role. For example, if the patch in **Figure 2** produced inhibitors instead of triggers, then larger patches would be OFF and smaller patches would be ON. Here we have focused on binary switches between two possible states, but the same reasoning also applies to biological systems that have more than two potential states, such as stem cells, which can remain pluripotent or differentiate into any of several different cell types.

State switching in response to patch size has been observed in several biochemical and cellular systems (**Figure 3**). For example, the enzymatic network of blood coagulation could be switched

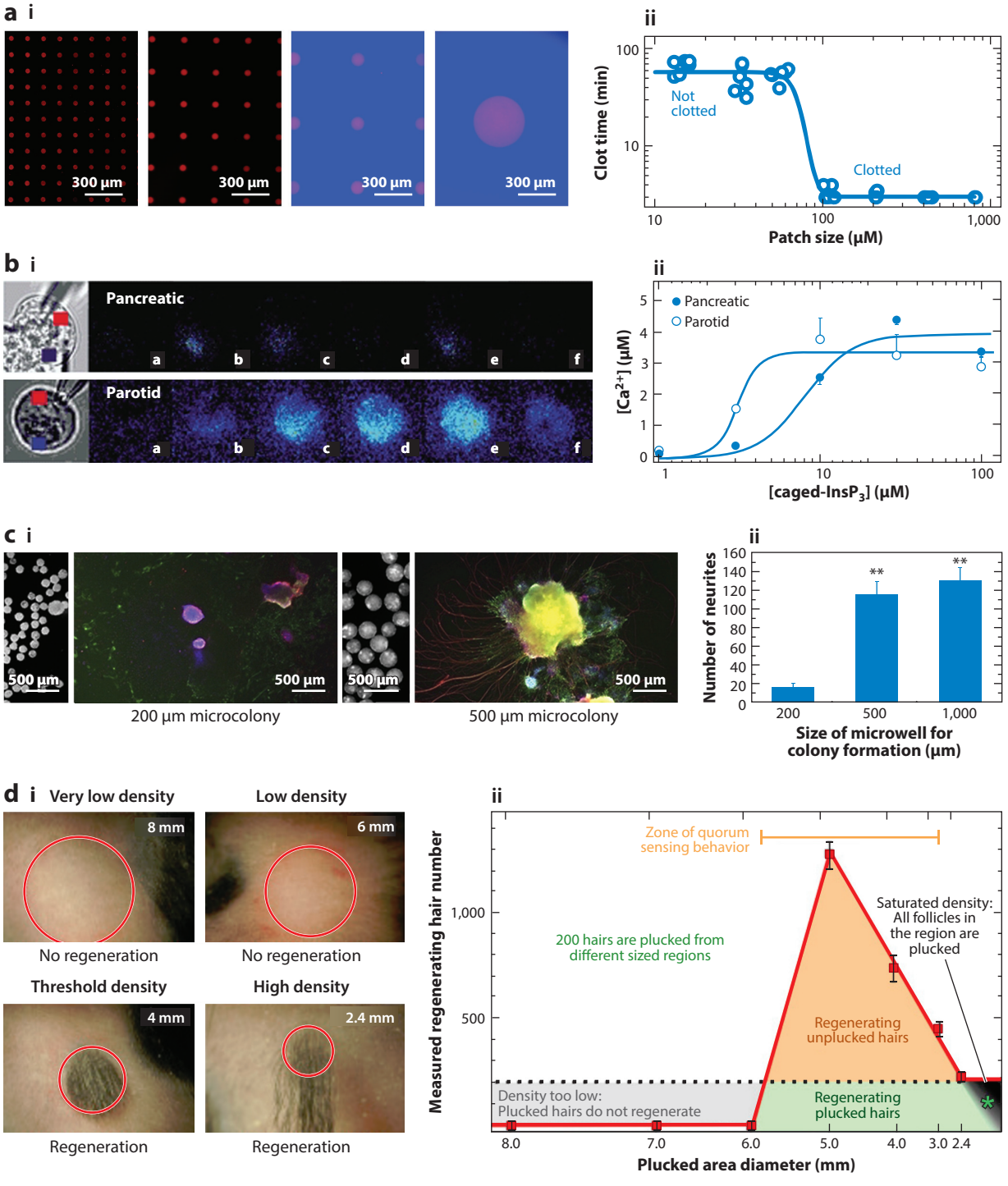

from a quiescent to a clotted state by increasing the size of micropatterned patches of TF, even though the total quantity of TF remained the same (**Figure 3*a***) (25). As discussed above, one expects to observe patchy switching in this network because there are threshold responses to soluble triggers involved in coagulation (12), such as the proteases thrombin (26) and factor Xa (11). Eukaryotic calcium signaling is another threshold-mediated system in which autocatalysis plays a role, and patchy switching has been observed here as well. Specifically, the ubiquitous intracellular inositol (1,4,5)-triphosphate ($IP_3$) receptor releases soluble $Ca^{2+}$ from the endoplasmic reticulum in response to above-threshold concentrations of $IP_3$ (27). This release drives a positive feedback loop in which the released $Ca^{2+}$ ions activate nearby $IP_3$ receptor clusters to release more calcium (28, 29). Interestingly, when soluble $IP_3$ was loaded at varying concentrations into murine pancreatic and parotid cells, $Ca^{2+}$ signals transitioned from small local spikes to global waves, a state change that depended on the density of $IP_3$ receptors in the cells (**Figure 3*b***) (30).

In another example, at larger scales, the direction of stem cell differentiation was shown to be potentiated by the size of stem cell embryoid bodies generated in microfluidic wells (3, 27). Studies by two independent groups have shown that small embryoid bodies remained inert to neurodifferentiation, whereas larger clusters (>250–350 μm in diameter) adopted a neural morphology with extensive neurite formation (**Figure 3*c***) (27, 31). The mechanism of this is still unclear and may or may not be due to diffusible signals, although the role of diffusible stem cell signals is being actively investigated (22, 32).

In the sections that follow, still using patchy switching as the example, we discuss recent developments in microfluidics and chemistry that provide experimental control over factors that affect the local balance (*Da*) of reactions (**Figure 4*a***) and transport (**Figure 4*b***), such as patch size, clustering, confinement, and the effects of flow and changing diffusivity.

## MICROSCALE CONTROL OVER TRANSPORT PHENOMENA

### Controlling Patch Size and Clustering

Changing the patch size, $x$, by patterning cells or molecules (while keeping their numbers constant) affects the *Da* number by changing the diffusion time of soluble triggers away from the patch, $\tau_D \sim x^2/D$ (**Figures 2*c*** and **4*b*,*i***). To help determine whether patchy switching plays a role in a system of interest, a wide range of tools, many based on photochemistry (33) and soft lithography (a range of biocompatible micropatterning techniques) (29), can be used to pattern molecules and cells onto in vitro surfaces (**Figure 5*a***) (34). Multiple molecular or cellular entities can be patterned separately or in close proximity to one another (**Figure 5*b*,*c***) (35–39), for example, to

**Figure 3**

Switching in response to changes in spatial distribution. (*a*, *i*) Blood coagulation (*blue*) is initiated on micropatterned patches of tissue factor (*red*) only if they are larger than a critical size, quantified in subpanel *ii*. Panel *a* adapted with permission from Reference 25, © 2006 National Academy of Sciences, USA. (*b*, *i*, *top*) Only localized $Ca^{2+}$ puffs were produced in response to local release of photocaged inositol (1,4,5)-triphosphate ($IP_3$) in murine pancreatic cells expressing low density of inositol trisphosphate receptors ($InsP_3R$); (*b*, *i*, *bottom*) global $Ca^{2+}$ (*blue*) waves were switched on in response to local release of photocaged $IP_3$ in murine parotid cells expressing high density of $InsP_3R$ (30). (*b*, *ii*) A plot showing that parotid cells have a lower threshold $IP_3$ concentration for maximum $Ca^{2+}$ release than the pancreatic cells. Panel *b* adapted from Reference 30 with permission. (*c*, *i*) Embryoid bodies preferentially differentiated into neural precursor cells (*green*) with long neurites (*red*, quantified in subpanel *ii*) only when they were at least 500 μm in size. Panel *c* adapted from Reference 27 with permission. (*d*, *i*) Plucking hairs on the skin of mice induced amplified hair regeneration only when hairs were plucked above a threshold density, quantified in subpanel *ii*. Red circles in images show the regions from which 200 hairs were plucked 30 days prior to the photo. Panel *d* adapted from Reference 63 with permission.

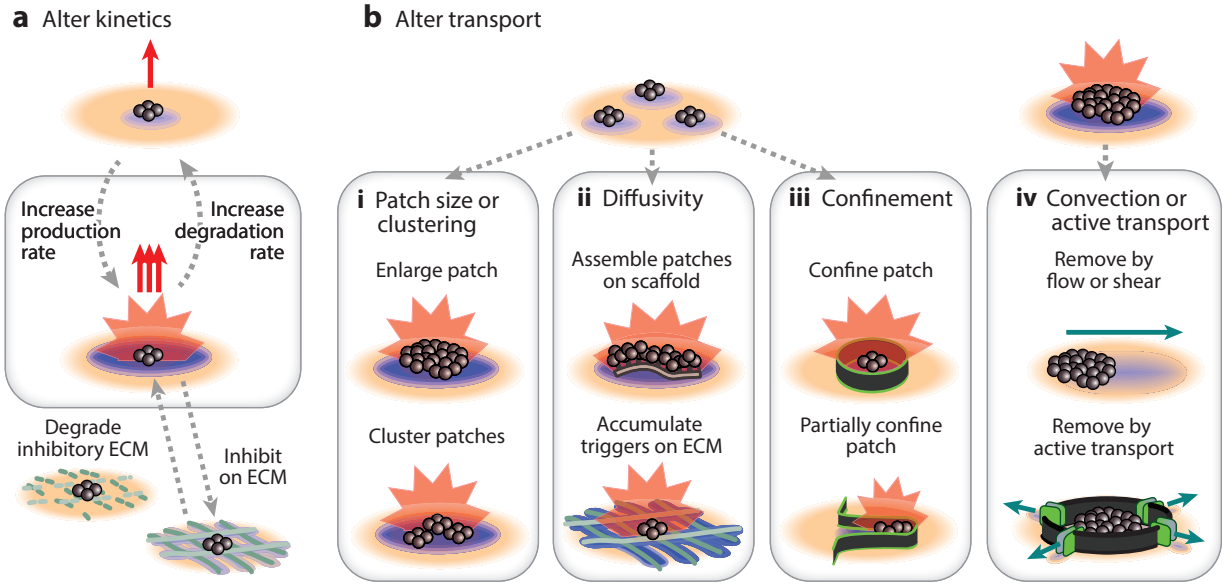


**Figure 4**

Various mechanisms for inducing patchy switching by changing the Damköhler number. (*a*) Altering the local concentration of a trigger (*blue*) by increasing its rate of production by the activators in the patch (*gray spheres*) can turn a system with threshold kinetics ON (*red starburst*). Inhibitory binding of a trigger on the extracellular matrix (ECM) also can turn the system OFF, whereas degrading the ECM can restore the ON state. (*b*) Altering transport (*i–iii*) by limiting diffusional flux increases the local concentration and can turn the system ON, whereas increasing removal (*iv*) by increasing the rate of convection or active transport (*green arrows*) decreases the local concentration and can turn the system OFF. Each of these processes can also occur in reverse.

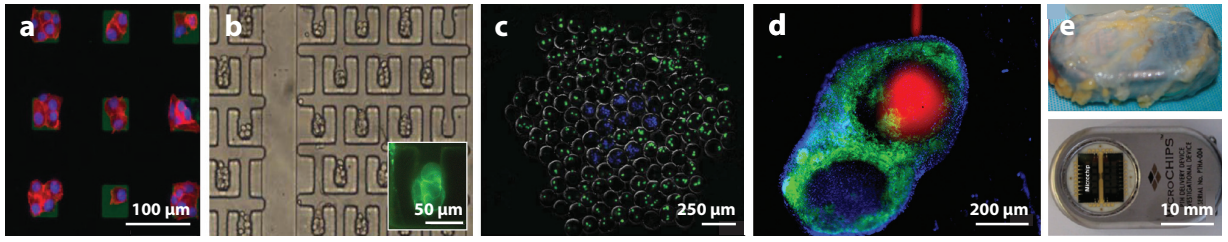


**Figure 5**

Controlling patch size and clustering using chemistry, microfluidics, and local drug delivery systems. (*a*) Two-dimensional patches of human oral squamous carcinoma cells micropatterned using a peel-off perylene stencil. Panel *a* reproduced from Reference 34 with permission. (*b*) Three-dimensional (3D) tumor spheroids formed and stained (*inset*, *green*) in microfluidic traps. Panel *b* adapted from Reference 37 with permission. (*c*) Two-dimensional chemical patterning of 3D microcultures containing rat fibroblasts (*green*) or human lung adenocarcinoma cells (*blue*) using DNA templates. Panel *c* reproduced from Reference 35 with permission. (*d*) Localized chemical stimulation (*red*) of a murine lymph node slice cultured in a microfluidic chamber. The slice was immunostained for B cells (*green*) and counterstained with Hoechst (*blue*), allowing specific regions to be targeted for stimulation. Panel *d* reproduced from Reference 53 with permission from The Royal Society of Chemistry. (*e*) Microchip implanted in a human to locally deliver discrete doses of a hormone fragment, which increased bone formation in women with osteoporosis. Panel *e* adapted from Reference 160 with permission.

study heterotypic interactions among patches (39). In addition to providing the ability to culture materials on two-dimensional (2D) surfaces, these micropatterning and microfluidic tools are well suited to the generation of size-controlled three-dimensional (3D) cultures of microtissues, tumor spheroids, and stem cell organoids (40). Microfluidic laminar flow is another simple way to control the spatial distribution of cells in 2D or 3D, often by patterning parallel lanes of cells, gels, and stimuli. Finally, true 3D patterning is now possible as a result of advances in biomaterials, chemistry, and 3D bioprinting, so that molecules and cells can be patterned on or within functionalized polymeric scaffolds or matrices for more realistic, tissue-like geometries (41–45). These patterning tools have been invaluable for evaluating the effect of patch size on blood coagulation (**Figure 3*a***) (25) and stem cell differentiation (**Figure 3*c***) (27, 31, 46–48). Patterning can also distinguish the role of cell–cell contacts from that of soluble signaling (28) to help assess the extent to which transport-mediated signals drive a particular system. For example, in a study of tumor invasiveness, a patterned coculture of mammary epithelial cells and human mammary fibroblasts was generated with and without a cell-free lane between them (49), revealing that the epithelial transition to an invasive phenotype was initiated by diffusible signals but required cell–cell contact to be completed.

In contrast to building patterned cell cultures, patchy distributions also can be created when preexisting in vitro cell cultures (50–52) or intact ex vivo tissue slices (**Figure 5*d***) (53–58) are locally stimulated using spatially resolved microfluidic delivery. Modern microfluidic designs that stimulate local regions of neuronal cells (59), essentially creating a patch on a subcellular level, have built on early work by pioneers such as Campenot (60). Delivery of soluble molecules or proteins to spatially structured cells and tissues has the potential to enable investigation of patchy switching and related dynamics, as described in the next paragraph.

We note that not all clusters are patches and not all spatial effects are due to the patchy switching mechanism described here. For example, even if large patches turn the system ON and small patches do not, a critical question is whether the effect is driven by greater accumulation of diffusible triggers (patchy switching as in **Figure 2*d***) or simply by having a larger quantity of the activator (not patchy switching). Microfluidic and micropatterning experiments provide the control needed to tease apart these differences. For example, a microfluidic device was used to deliver a potassium chloride solution to local regions of murine brain slices, causing the cortical spreading depressions that simulate a migraine (58). By varying the radius of the delivery region and the concentration of potassium, the researchers showed that it was the total quantity of potassium, not the area over which it was spread, that determined whether spreading depressions occurred (61). A response to a larger quantity of activator is not the same as a response to its spatial distribution and does not require nonlinear kinetics. The result of this potassium stimulation experiment contrasts with the patchy switching observed for blood clotting when TF was micropatterned into patches of varying sizes while holding the total quantity constant (**Figure 3*a***).

Clustering of patches and variations in patch density are other mechanisms that can change the *Da* number and induce switching (**Figure 3*b*, *i***). As patches are brought closer together, diffusion of triggers from one patch overlaps with diffusion of triggers from nearby patches, and ultimately closely spaced small patches functionally merge together. On the molecular scale, self-assembly of signaling molecules on scaffolds (62) is a remarkable example of clustering. Tethering diffusing enzymes and substrates to a scaffold can raise the effective local concentration substantially; such clustering can alter propagation of information through signaling pathways (62) and could lead to switching. Clustering can play a role at the tissue scale as well and can have marked effects on organ-level function. For example, a link was made recently between clustering-induced patchy switching and stimulated hair regrowth. Specifically, plucking a few hairs from the back of a mouse caused robust hair regrowth but only if the hairs were plucked above a threshold density

(**Figure 3*d***) (63). The effect was mediated by local transport and accumulation of inflammatory proteins.

The micropatterning techniques described above make it easy to test the effect of clustering in vitro. For example, in blood coagulation, micropatterning was used to generate clusters of subthreshold patches of *Bacillus* bacteria on an otherwise inert surface. When human blood plasma was exposed to these surfaces, unclustered patches of *Bacillus* did not initiate clotting, but clustered patches induced a robust coagulation response (64). These experiments demonstrated that a bacterial species could initiate the full coagulation cascade via a quorum acting mechanism, and the work identified a bacterial zinc metalloprotease InhA1 as the activator of human thrombin and factor Xa. Controlled clustering or localization of cells has also been used to study the complex effects of autocrine and paracrine signaling, for example, to separate the effects of cell–cell contact and soluble signaling on the liver-specific function of hepatocyte–stromal cocultures (65) or on colony formation by murine embryonic stem cells (66).

Tools are also emerging to test the role of spatial distribution and patches in vivo, in the context of immune responses, the growth of tumors, and the local effects of xenografts or subcutaneous vaccinations. Microfluidic tools are potentially more invasive than optical probes and need to be refined to be used deep in tissues in vivo (67, 68). Genetic manipulation can be used to create patchy distributions by utilizing temporally and spatially specific promoters or by creating chimeric or mosaic animals—for example, in a chimeric mouse model of amyotrophic lateral sclerosis (69), although it is not known whether patch size plays a role in this system. In vivo patches of controlled sizes can be created by microneedles, grafting, ultrasound, insertion of artificial tissue scaffolds and hydrogels, and local drug delivery systems (3, 70–74). In mouse models of ischemic injury, for example, local hydrogel-mediated delivery of vascular endothelial growth factor (VEGF) and insulin-like growth factor-1 (IGF1) in tandem resulted in increased muscle weight. Such experiments suggest that spatial and temporal control play a key role in revascularization and regeneration in vivo (71, 75). Numerous other local drug delivery systems are being developed that could be used to create large patches. The goal of most drug delivery systems is to maintain a sufficiently high local concentration of a therapeutic drug in the target tissue while using low and safe total amounts of the drugs; however, these systems could be extended to test the role of patches in vivo. Light can also be used to create patches in vivo. Laser-induced injury of blood vessels (76) is used extensively to create patches of damaged vasculature and initiate blood coagulation; however, this technique has not yet been used to test if patchy switching occurs during initiation of coagulation in vivo. Dynamically, patches of cells can be created and switching can be induced in vivo using optogenetics (77), dynamic patterning (36), and possibly the microfluidic tools for local chemical stimulation described above.

## Chemically Controlling Diffusivity

Another method to induce patchy switching is to chemically reduce the diffusivity, $D$, of triggers causing them to accumulate locally (**Figure 4*b*, *ii***). Diffusion of triggers can be restricted by binding them to or incorporating them into large, low-mobility objects such as proteins, vesicles, and exosomes (78) or by oligomerization and fibril formation. For example, intracellular binding of $Ca^{2+}$ ions to soluble calcium-binding proteins enables local accumulation of $Ca^{2+}$ and promotes initiation of global calcium waves (79). Furthermore, binding of trigger molecules to nondiffusing objects, such as cell surfaces, intracellular scaffolds, or the ECM, further reduces the effective diffusion coefficient. For example, during coagulation in a damaged blood vessel, activated enzymes bind to the area of exposed endothelium and aggregated platelets, which raises their local concentration and amplifies the cascade (12, 80). In the context of tissue growth and repair as well

as inflammation, many cytokines, chemokines, and growth factors bind to proteoglycans on cell surfaces or to components of the ECM, which limits diffusive loss and enables local chemoselective accumulation despite constant interstitial, vascular, or lymphatic flow (3, 5, 73, 81–83). The ECM and closely packed cell bodies also reduce diffusivity by decreasing the free volume of the tissue, increasing tortuosity, and introducing sieving (84). Reduced diffusion through the ECM is well established for a variety of systems including ischemic injuries (85), brain tissue (86, 87), tumor microenvironment (84, 88, 89), mucosal linings in the gut and other organs (90), bacterial biofilms (91), fibrosis on implanted materials (92), and stem cell embryoid bodies (93). In addition to reducing the diffusion of triggers, binding to the ECM may change their chemical or functional properties, for example, by protecting chemokines and cytokines from enzymatic degradation or preventing binding to cellular receptors (1, 94). Modifying the trafficking of molecules into and out of cells is another biological mechanism for controlling transport and switches and occurs, for example, by regulating endocytosis (95). Controlled uptake of chemokines, for example, has been shown to allow cells to create their own chemotactic gradient for self-directed migration (96).

Tools are emerging to manipulate diffusion chemoselectively by altering binding events. Both the signaling proteins [e.g., chemokines (82, 97, 98)] and the ECM (2, 4, 73, 97, 99) have been modified in vitro and in vivo, yielding insights into the roles of restricted diffusion. For example, mutations in the glycosaminoglycan (GAG)-binding sites of three chemokines, monocyte chemoattractant protein-1/CCL2, macrophage inflammatory protein-1β/CCL4, and RANTES (regulated on activation normal T cell expressed and secreted)/CCL5, were designed to prevent binding of the chemokines to heparan sulfate (82, 98). Although these mutants were chemoattractive in static in vitro conditions, they failed to recruit cells after injection into the peritoneal cavity in mice, thus confirming that GAG binding is essential for proper spatial localization and function of these chemokines in vivo. Decreased diffusion can be engineered as well; for example, TG-VEGF, a VEGF variant with an amino-terminus factor XIIIa substrate sequence, was designed to bind directly to fibrin in blood clots and fibrin glue tissue sealants, raising the local VEGF concentration long enough to enhance angiogenesis (2). To engineer the ECM, proteins or hydrogels have been designed to present specific binding motifs for soluble factors (73, 100). For example, a fibrin matrix was engineered to express a chemokine-binding motif, the twelfth–fourteenth type III repeats of fibronectin (FN III12–14); this matrix slowed diffusive loss of platelet-derived growth factor-BB and increased tissue growth responses (4). Accumulation of soluble factors is distinct from presentation of cell-binding motifs such as RGD (arginylglycylaspartic acid); however, chemokine- and integrin-binding motifs can certainly function synergistically as well (101, 102). The ability of microfluidics to pattern and deliver reagents brings spatial resolution to diffusion experiments. Microfluidics and micropatterning can also be used to pattern ECM proteins (**Figure 6*a***) (103, 104), inhibitors of binding, or other molecules (e.g., affinity reagents and receptors, and size-selective or chemo-selective matrices) that can help control diffusivity. As described above, microfluidic tools also enable local delivery of reagents, which can be used to measure diffusion through the ECM or measure transport in even more complex systems such as gap junctions (105), to provide insights into mechanisms of transport and switching.

## Utilizing Confinement

A complementary approach to changing *Da* to induce patchy switching is restricting diffusion using geometric constraints, such as physical confinement (**Figure 4*b*, *iii***). Confinement promotes the accumulation of secreted molecules and can raise the local concentration of triggers above the threshold value, inducing switching. Confinement of diffusible triggers is common in nature and is the basis for vesicles, organelles, cells, and other biological compartments. Experimentally,

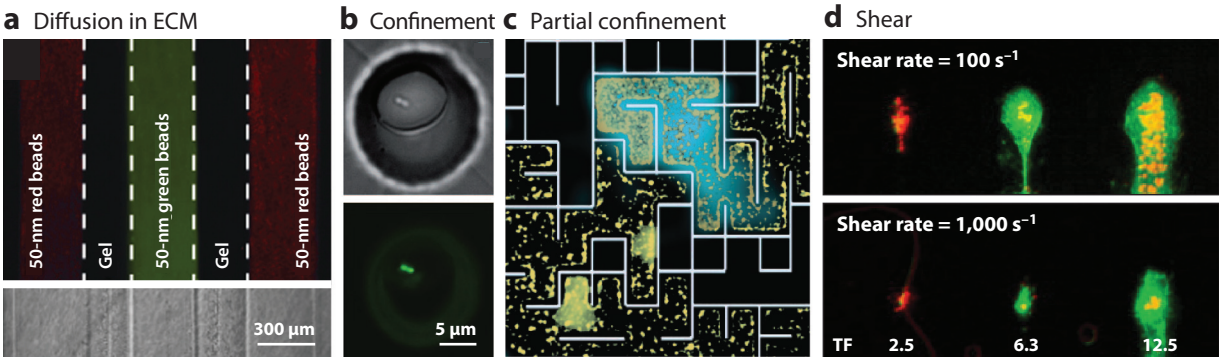


**Figure 6**

Microfluidic control over confinement and flow near patches. (*a*) Microfluidic patterning of the extracellular matrix (ECM) using Matrigel with distinct spatial zones visible by fluorescence (*top*) and phase contrast imaging (*bottom*). Panel *a* adapted from Reference 103 with permission. (*b*) Confinement of single cells or small groups of *Pseudomonas aeruginosa* in ~0.1 pL droplets activated a fluorescent reporter for the quorum sensing–controlled gene *lasB* (*green fluorescence*). Panel *b* adapted from Reference 111 with permission. (*c*) Partial confinement of motile *Vibrio harveyi* (*yellow*), initially loaded uniformly in a microfluidic maze (*white lines*) with 100 μm passages, caused accumulation of cells and activation of quorum sensing (*blue luminescence*) in partially confined regions of the maze. Panel *c* adapted from Reference 120 with permission. (*d*) Increased shear of whole blood over patches of collagen and tissue factor (TF) prevented propagation of a fibrin (*green*) and platelet (*red*) clot over the middle patch. Panel *d* adapted from Reference 126 with permission.



synthetic analogs of these structures include nanoscale lipid structures (106, 107) and microfluidic femto- to picoliter aqueous droplets or chambers (108–110).

In the past five to ten years, the role of confinement in inducing state changes has been explored extensively in the context of bacterial quorum sensing. In 2009, microfluidic confinement in picoliter volumes induced quorum sensing in a single cell or a few cells of *Pseudomonas aeruginosa*, presumably because of accumulation of autoinducer molecules in the confined volume (**Figure 6*b***) (111). This finding was later confirmed using other microfluidic strategies to confine cells of *P. aeruginosa* (112), *Staphylococcus aureus* (113), and *Vibrio fischeri* (114). These systems may be used to mimic the confinement that may occur during endocytosis of microbes and mimic the dynamics of intracellular pathogens. In an interesting model of engulfment of *Mycobacterium tuberculosis* by macrophages, microfluidic confinement of mycobacteria in small volumes (5 cells in 200 pL, or $\sim 2 \times 10^7$ cells/mL) was sufficient to induce antibiotic resistance (115). This effect was not seen in larger volumes and suggests that a quorum sensing–like mechanism is at work. Full confinement of mammalian cells could facilitate studies of autocrine and paracrine signaling, but the duration of confined culture is limited to just a few hours by the damaging effects of nutrient depletion and the accumulation of cellular waste products (116). Strategies that alternate periods of full confinement with interludes of media exchange (115) may circumvent these effects and enable confinement-based studies on mammalian cells.

Partial confinement—when a patch is confined but not in every direction—also restricts diffusion and leads to effective accumulation of signals while reducing the accumulation of waste products. Natural architectures such as intercellular spaces (117), intestinal crypts (118), or cortical sulci (119) may lead to partial confinement and accumulation of molecules or cells in that space. Therefore, this approach is well suited to mammalian as well as bacterial in vitro cell culture. Microfluidics has been used to mimic conditions of geometric partial confinement in quorum sensing and blood clotting (120–122), showing that state switching can occur even in the presence of limited diffusion or flow. For example, soft lithography was used to generate maze-like

microfluidic geometries that were then filled with liquid cultures of motile *Vibrio harveyi*. The microbes were initially distributed uniformly, but after 1–3 h they accumulated in the dead ends of the maze and activated quorum-dependent responses, presumably responding to accumulating autocrine signals in partially confined regions (**Figure 6*c***) (120). Furthermore, when compressive stress was used to decrease intercellular space in cultures of endothelial cells, it enhanced autocrine epidermal growth factor (EGF) signaling and increased EGF receptor activation equivalent to a 10-fold increase in soluble EGF (117). These results show that confinement is especially effective for activating signaling that incorporates positive feedback loops, including autocatalysis in blood coagulation, or autocrine EGF signaling and quorum sensing. Partial confinement would be particularly effective in combination with chemoselective confinement by the ECM, which would capture triggers such as cytokines or growth factors while letting nutrients and waste pass through unhindered. Existing patterning tools can be combined with chemistry to decorate the ECM with binding functionalities (44) or to use the sieving (84) effects of ECM to study the effects of chemoselective confinement on patchy switching.

## Manipulating Flow and Shear

Fluid flow provides another way to induce switching by changing the local concentration of soluble triggers, by either delivering them to a patch or washing them out (**Figure 4*b*, *iv***). In solution or in bulk tissue, flow is best described by the linear flow velocity, $V$ (meters per second). Near a surface, such as the endothelium, the effectiveness of transport is best described by the shear rate, $\dot{\gamma} = V/L$ (seconds$^{-1}$), where $L$ is a characteristic length (meters) over which the flow velocity is changing, such as the radius of a microfluidic channel or blood vessel. Shear rate controls the dynamics in systems such as blood coagulation (123), and its effects on transport are distinct from shear-induced mechanical stress that can also induce signaling processes.

How does one know whether diffusion or flow is more important to transporting triggers in a particular system? The relative contributions of flow and diffusion to transport of a trigger are quantified by a dimensionless quantity termed the Péclet number: $Pe = LV/D$. At high $Pe$ ($Pe \gg 1$), flow dominates, whereas at low $Pe$ ($Pe \ll 1$), diffusion dominates. However, often the two work in concert: The combination of flow and diffusion generates gradients, so that the effect of flow extends beyond where the flow actually is (83). For example, in solid tumors, flow through vessels delivers oxygen and nutrients that then diffuse to generate regions of proliferating tissue surrounded by hypoxic and then necrotic tissue (124). A similar mode of transport occurs within biofilms (91). Hydrostatic pressure from blood flow drives slow interstitial flow (0.1–2 μm/s) through soft tissues, which redistributes soluble molecules into gradients (83). Incorporating these flows into tissue-engineered models is essential to recreating biological functions such as chemotaxis (81).

Microfluidic techniques are well suited to controlling fluid flow in vitro at the size and volume scales most relevant to patchy switching and are already being exploited for this purpose (125). For example, microfluidic tools have been used to test the effects of flow and shear on the initiation of blood coagulation and platelet activation (**Figure 6*d***). When human whole blood or plasma flowed through microfluidic channels over surface-patterned patches of TF, the coagulation cascade switched ON only when low shear rates were used (126, 127). Bacterial quorum sensing has also been tested for its response to flow. In one experiment, 3D picoliter lobster traps were fabricated inside a microchannel by cross-linking the protein bovine serum albumin (BSA) (112), and *P. aeruginosa* bearing a fluorescent reporter for quorum sensing was cultured inside the trap. Quorum sensing was then induced simply by lowering the flow rate of media over the trap, indicating the sensitivity of this behavior to the transport conditions around the colony.

Microfluidic flow has also been used to control state switching in mammalian cell cultures, often by using controlled perfusion to wash out autocrine or paracrine cell-secreted factors. Such a system was used to probe the mechanism of autocrine signaling by mouse embryonic stem cells in maintaining a self-renewing state (22). Gentle perfusion over the cells induced a shift away from self-renewal into an epiblast state, apparently not by simply removing autocrine growth factors but by removing secreted matrix-remodeling factors such as matrix metalloproteases (22). This experiment illustrates the impact of both flow and ECM binding in cell fate decisions. Flow has also been used to control directional heterotypic cell–cell interactions, as has been reviewed previously (39). Recently, an elegant microfluidic device design combined control over interstitial flow with control over flow-mediated paracrine signaling; endothelial cells seeded into the device switched into vessel formation only when paracrine signals were present (128). Combining microfluidics with biomaterials to control diffusion and flow simultaneously provides an opportunity to mimic in vitro complex biological gradients (129) and test the effects of slow interstitial flow (130). Tools to modify the transport of molecules and induce flow are also being developed. For example, micromotor and self-propelling particles are being developed to actively transport their cargo in vitro and in vivo. Self-propelling particles have been used to transport triggers of coagulation against flow and deep into wounds to treat severe hemorrhage in large animals (131). Micromotors have been used to transport drugs throughout gastric acid in the stomach (132) and to transport their cargo into target cells (133).

## CONCLUSIONS AND OUTLOOK

### To Which Biological Systems Might Patchy Switching Apply?

The tools discussed here may provide the greatest insights for biological systems with the hallmark characteristics of patchy switching—in other words, those that display spatial heterogeneity, are driven by diffusible signals, show highly nonlinear (e.g., threshold) responses to those signals, and are influenced by factors that affect mass transport, such as flow, partial confinement, changes in clustering or patch size, and binding to the ECM. Many systems meet most or all of these criteria. For example, inflammation is a highly nonlinear process that is driven by the local concentration of cell-secreted cytokines (134); both the cells and the cytokines are mobile and respond to diffusion, interstitial flow, clustering and confinement in tight spaces, and binding to the ECM (135). Cellular decisions in stem cell niches, cancer niches, developmental niches, sites of wound healing, sites of chronic inflammation, and even bacterial biofilms are similarly dependent on the spatial distribution of secreted factors that interact with the microenvironment in multiple ways. Furthermore, many of these systems include positive feedbacks, which could lead to spatial propagation of the switched state (**Figure 3*a***) and also to stabilization of one state against perturbations. We call this stabilization state imprinting. In niches (e.g., stem cell niches, cancer niches, developmental niches) in particular, such stabilization could occur from extensive interactions between the cells and the ECM (20, 21), during which a patch of cells that has undergone a state switch can modify the surrounding ECM to change its affinity for soluble signals and further stabilize the state against perturbations, effectively converting a transient switching event to a chronic one.

### Case Study: Possible Patchy Switching in the Lesions of Multiple Sclerosis

At first glance, it may seem that real biological systems are much too intricate to map onto the patchy switching paradigm. Therefore, it is worth examining a case study. To discuss one example, we turn to localized inflammation in the demyelinating lesions of multiple sclerosis (MS),

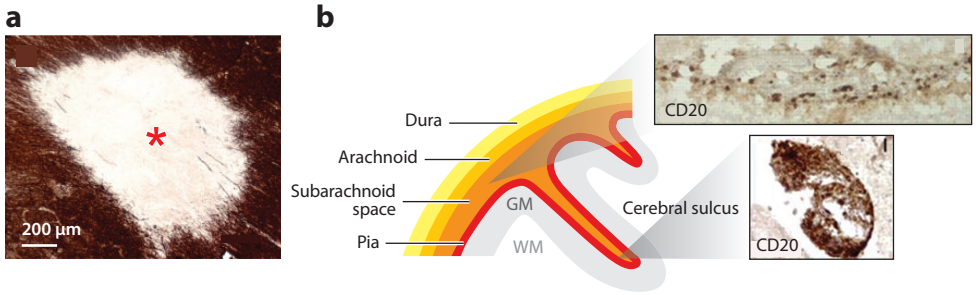


**Figure 7**

Lesions and ectopic follicles in multiple sclerosis (MS) are candidates for patchy switching. (*a*) Focal demyelinated lesions in the white matter (161) appear consistent with a response to patch size and clustering. The asterisk indicates the center of the lesion identified by the absence of brown staining for proteolipid protein, a component of myelin. Panel *a* adapted from Reference 161, available under the Creative Commons Non-Commercial 2.0 UK License (**http://creativecommons.org/licenses/by-nc/2.0/uk/**). (*b*) Ectopic B cell follicles located deep inside cortical sulci in secondary progressive MS are consistent with patchy switching in response to confinement of inflammatory signals. The schematic details the geometry of a cerebral sulcus, including the three layers of the meninges (dura, arachnoid, and pia mater). Insets: Immunohistochemistry for B cells (CD20, *brown*) revealed follicles located inside the sulcus but not at the external surface of the brain. Panel *b* adapted from Reference 119 with permission. Abbreviations: GM, gray matter; WM, white matter.



which appears to satisfy the criteria for patchy switching as well as propagation and imprinting of the switched state. In the white matter, lesions are often arranged focally around a central vein or capillary, and active lesions include a radially symmetric influx of activated macrophages and myelin-specific T cells that are associated with loss of myelin (**Figure 7*a***) and axonal damage (136). Spatially, these lesions show focal activation and radial propagation, reminiscent of initiation of blood clotting over surface-patterned TF patches (**Figure 3*a***) (25). In the gray matter, demyelinating lesions are commonly adjacent to cortical sulci, which can contain ectopic B cell follicles that persist deep inside the sulcus (**Figure 7*b***) (119) and may serve as a confined source of inflammatory mediators (136). Like other neuroinflammatory diseases, MS lesions may be driven by nonlinear responses because neurodegeneration and inflammation together drive a positive feedback loop (137) that propagates and possibly state imprints tissue damage.

We speculate that demyelinating MS lesions may undergo patchy switching in response to large patch size and clustering (in the white matter), limited diffusion in the inflamed extracellular space, and confinement of inflammatory signals (for follicles in the sulci). The signals driving the feedback loop may include the products of myelin degradation, secretion products from activated microglia and immune cells, and/or matrix components, such as fibrinogen (136, 138, 139). A threshold may be present as well, set by clearance of these signals and inhibition of immune response by regulatory systems. Numerous small prereactive clusters of activated microglia, associated with precipitated fibrin but without accompanying demyelination, have been observed in MS autopsy tissue (139, 140). If formation of lesions in MS was controlled by patchy switching, these prereactive lesions could be viewed as subthreshold patches that did not trigger the inflammatory positive feedback loop (analogous to subthreshold TF patches unable to trigger blood coagulation in **Figure 3*a*, *i***). How might these predictions be tested experimentally? De novo recapitulation of neuroinflammation is beyond the current capabilities of cell patterning and microfluidic devices, despite exciting developments in the organ-on-a-chip field (141). However, recent advances in microfluidic culture and local chemical stimulation of intact brain slices (57, 58) could be used to

test whether patchy switching can drive the onset of local inflammation ex vivo. For example, a localized pulse of cytokines or myelin degradation products could be delivered to a rodent brain slice in arrays of focal regions of varying size. The first prediction is that for a given concentration of trigger, inflammatory monocytes or lymphocytes would be recruited only when the local delivery regions exceeded a critical size. The second prediction is that recruitment takes place, and the switch to the inflammatory state would persist and propagate outward.

## Outlook on Tools for Testing the Role of Patchy Switching In Vitro and In Vivo

Knowing that a system of interest is undergoing patchy switching is invaluable because it allows one to use *Da* as a unifying framework to predict how switching dynamics may be affected by changes in the many factors that affect transport rates (**Figure 4**). Obviously, not all systems that appear patchy or satisfy the criteria for patchy switching would actually show patchy switching. For example, if relative transport and reaction rates differ drastically or the threshold is too far from the resting value, small changes in reaction or transport rates may be insufficient to cross the critical value of *Da*. Furthermore, alternative mechanisms (81) such as mechanotransduction (142) and cell–cell (49, 141) and cell–matrix contacts (142) would in most cases influence the range of parameters in which patchy switching could occur and, in some cases, would dominate over effects of diffusible signaling and *Da* number. Thus, to confirm or disprove patchy switching in each system of interest, one needs to measure and modulate transport rates and the spatial distribution of potential trigger molecules using a chemically selective approach. Microfluidic and chemical tools are essential to accomplish this.

In vitro, some of the microfluidic tools we have discussed in this review are still at the proof-of-concept stage, and few are sufficiently robust for use by nonexperts, although they are potentially available through collaboration with microfluidics laboratories. But some microfluidic tools are now commercially available and are producing biological insights, and other tools are likely to mature rapidly toward widespread use. We expect the use of these tools to increase as advances are made in tissue engineering and in other techniques that enable complex processes to be validated ex vivo and in vitro.

In vivo and ex vivo, additional spatially resolved analytical tools are urgently needed and have begun to appear recently. For measurements with high spatial, temporal, and chemical resolution, microsampling techniques combined with off-line analysis (50–52, 143) could be utilized but are invasive (144). In vivo electrochemistry with probes a few micrometers in diameter can provide information on electroactive molecules; this technique has been particularly useful in brain research (145) and may also become useful in immunity research (146). Imaging approaches are naturally spatially resolved, and confocal and two-photon imaging techniques in live tissue (147) are becoming increasingly accessible to nonspecialist researchers. Optical imaging, as well as positron emission tomography (PET), functional magnetic resonance imaging (fMRI), and diffusion MRI techniques, can be done noninvasively but require that chemical wash-in, wash-out, or caged probes be developed for each molecule of interest (148, 149). Genetically encoded probes for MRI and ultrasound techniques (150, 151) are particularly intriguing for noninvasively monitoring biological processes in vivo. Spatially resolved analysis of RNA and protein expression is particularly exciting and has been called for recently (152).

Once developed, methods for spatially resolved analysis in vivo will be useful for identifying niches that chemoselectively accumulate or lose trigger molecules and also for visualizing the activity of the cells and remodeling enzymes responsible for creating such niches. Furthermore, such methods could identify regions of confinement and chemoselective confinement as well as changes

in local flow, and these methods could be used to measure the size of patches, identify clusters of patches, and monitor their switching. Such tools could also improve basic understanding of in vivo transport rates; how they are affected by matrix composition; how they change with inflammation, stress, disease, aging, and physical activity; and how they affect patchy switching in vivo. Diagnostically, such tools could support early detection and monitoring of treatment by identifying subthreshold, near-threshold, and above-threshold patches and corresponding niches—for example, by identifying early fibrinogen deposits in MS or precancerous lesions in sites predisposed to cancer (20)—or by monitoring sites of chronic inflammation.

Creating patches and controlling rates of transport to control switching in vivo are even more challenging than analyzing them, but progress has been made in developing tools that can do so. Creating patches of known sizes could potentially be accomplished by using optogenetic techniques based on model organisms (153) or light-activated probes (154, 155), either of which provide a resolution of ~0.2–2 μm depending on tissue thickness and optical conditions. Alternatively, patches could be created by using focused ultrasound (resolution of a few millimeters) (156), or the more invasive microfluidic tools (resolution of tens of micrometers to millimeters) (143, 157). In terms of controlling transport, flow is a powerful factor to control switching, and methods to control local flow rates of blood, as well as interstitial, cerebrospinal, lymph, and synovial fluids, are still needed. Approaches are also particularly needed for chemoselective local synthesis, degradation, or modification of ECM, which would provide control over the binding of triggers to ECM in patches, and would allow one to modify, create, or erase patches and niches. To meet this need, synthetic biomaterials, delivered to specific spatial areas, could act as niches and provide control of diffusion in a chemoselective fashion. Their effects could be enhanced further using partial confinement approaches (e.g., mimicking the ectopic follicles in **Figure 7*b***) to promote switching. Such approaches could be used to create synthetic preimprinted niches with geometric, cytokine-binding, and transport properties suitable for initiation and propagation of a desired response and have been applied in a few promising models of adaptive immunity (158, 159). Similar niches are needed to allow controlled initiation of other processes such as neuroinflammation and wound healing. We speculate that methods for chemoselective control of transport in vivo also could be applied therapeutically to erase pathological microenvironments (e.g., prereactive lesions in MS or premetastatic niches in cancer) or create supportive microenvironments (e.g., in wound healing, tissue regeneration, or vaccination). Overall, the emerging spatially resolved tools, together with advances in understanding of biological complexity, make this an exciting time to study and manipulate patchy switching and related biological phenomena in nonlinear networks that are controlled by the balance of transport and reaction rates.

## DISCLOSURE STATEMENT

The authors are not aware of any affiliations, memberships, funding, or financial holdings that might be perceived as affecting the objectivity of this review.

## ACKNOWLEDGMENTS

This work was supported in part by a National Institutes of Health Director's Pioneer Award (DP10D003584, R.F.I.), a Jacobs Institute for Molecular Engineering for Medicine Award (R.F.I.), a National Science Foundation Emerging Frontiers in Research and Innovation Award (1137089, R.F.I.), an Individual Biomedical Research Award from The Hartwell Foundation (R.R.P.), and a Canadian Institutes of Health Research Award (MSH-130166, C.J.K.). We thank Natasha Shelby for contributions to writing and editing this manuscript.

## LITERATURE CITED


1. Tayalia P, Mooney DJ. 2009. Controlled growth factor delivery for tissue engineering. *Adv. Mater.* 21:3269–85
2. Ehrbar M, Zeisberger SM, Raeber GP, Hubbell JA, Schnell C, Zisch AH. 2008. The role of actively released fibrin-conjugated VEGF for VEGF receptor 2 gene activation and the enhancement of angiogenesis. *Biomaterials* 29:1720–29
3. Lee K, Silva EA, Mooney DJ. 2011. Growth factor delivery-based tissue engineering: general approaches and a review of recent developments. *J. R. Soc. Interface* 8:153–70
4. Martino MM, Hubbell JA. 2010. The 12th-14th type III repeats of fibronectin function as a highly promiscuous growth factor-binding domain. *FASEB J.* 24:4711–21
5. Dowd CJ, Cooney CL, Nugent MA. 1999. Heparan sulfate mediates bFGF transport through basement membrane by diffusion with rapid reversible binding. *J. Biol. Chem.* 274:5236–44
6. Tyson JJ, Chen KC, Novak B. 2003. Sniffers, buzzers, toggles and blinkers: dynamics of regulatory and signaling pathways in the cell. *Curr. Opin. Cell Biol.* 15:221–31
7. Pickup M, Novitskiy S, Moses HL. 2013. The roles of TGFβ in the tumour microenvironment. *Nat. Rev. Cancer* 13:788–99
8. Åström KJ, Murray R. 2003. *Feedback Systems: An Introduction for Scientists and Engineers*. Princeton, NJ: Princeton Univ. Press
9. Phillips R, Kondev J, Theriot J. 2008. *Physical Biology of the Cell*. New York: Garland Science
10. Fogelson AL, Neeves KB. 2015. Fluid mechanics of blood clot formation. *Annu. Rev. Fluid Mech.* 47:377–403
11. Jesty J, Beltrami E. 2005. Positive feedbacks of coagulation: their role in threshold regulation. *Arterioscler. Thromb. Vasc. Biol.* 25:2463–69
12. Mann KG, Brummel K, Butenas S. 2003. What is all that thrombin for? *J. Thromb. Haemost.* 1:1504–14
13. Rana K, Neeves KB. 2016. Blood flow and mass transfer regulation of coagulation. *Blood Rev.* 30:357–68
14. Epstein IR, Showalter K. 1996. Nonlinear chemical dynamics: oscillations, patterns, and chaos. *J. Phys. Chem.* 100:13132–47
15. Turing AM. 1952. The chemical basis of morphogenesis. *Philos. Trans. R. Soc. B* 237:37–72
16. Luss D, Sheintuch M. 2005. Spatiotemporal patterns in catalytic systems. *Catal. Today* 105:254–74
17. Holmes EE, Lewis MA, Banks JE, Veit RR. 1994. Partial differential equations in ecology: spatial interactions and population dynamics. *Ecology* 75:17–29
18. Okubo A, Levin SA. 2001. *Diffusion and Ecological Problems: Modern Perspectives*. New York: Springer
19. Saltzman WM, Olbricht WL. 2002. Building drug delivery into tissue engineering design. *Nat. Rev. Drug Discov.* 1:177–86
20. Bissell MJ, Hines WC. 2011. Why don't we get more cancer? A proposed role of the microenvironment in restraining cancer progression. *Nat. Med.* 17:320–29
21. Lu P, Weaver VM, Werb Z. 2012. The extracellular matrix: a dynamic niche in cancer progression. *J. Cell Biol.* 196:395–406
22. Przybyla LM, Voldman J. 2012. Attenuation of extrinsic signaling reveals the importance of matrix remodeling on maintenance of embryonic stem cell self-renewal. *PNAS* 109:835–40
23. Epstein IR. 1995. The consequences of imperfect mixing in autocatalytic chemical and biological systems. *Nature* 374:321–27
24. Runyon MK, Kastrup CJ, Johnson-Kerner BL, Ha TG, Ismagilov RF. 2008. Effects of shear rate on propagation of blood clotting determined using microfluidics and numerical simulations. *J. Am. Chem. Soc.* 130:3458–64
25. Kastrup CJ, Runyon MK, Shen F, Ismagilov RF. 2006. Modular chemical mechanism predicts spatiotemporal dynamics of initiation in the complex network of hemostasis. *PNAS* 103:15747–52
26. Pompano RR, Li HW, Ismagilov RF. 2008. Rate of mixing controls rate and outcome of autocatalytic processes: theory and microfluidic experiments with chemical reactions and blood coagulation. *Biophys. J.* 95:1531–43
27. Choi YY, Chung BG, Lee DH, Khademhosseini A, Kim JH, Lee SH. 2010. Controlled-size embryoid body formation in concave microwell arrays. *Biomaterials* 31:4296–303

28. Bhatia SN, Balis UJ, Yarmush ML, Toner M. 1999. Effect of cell–cell interactions in preservation of cellular phenotype: cocultivation of hepatocytes and nonparenchymal cells. *FASEB J.* 13:1883–900
29. Xia Y, Whitesides GM. 1998. Soft lithography. *Annu. Rev. Mater. Sci.* 28:153–84
30. Giovannucci DR, Bruce JIE, Straub SV, Arreola J, Sneyd J, et al. 2002. Cytosolic $Ca^{2+}$ and $Ca^{2+}$-activated $Cl^-$ current dynamics: insights from two functionally distinct mouse exocrine cells. *J. Physiol.* 540:469–84
31. Chen Y-H, Peng C-C, Tung Y-C. 2015. Flip channel: a microfluidic device for uniform-sized embryoid body formation and differentiation. *Biomicrofluidics* 9:054111
32. Przybyla LM, Theunissen TW, Jaenisch R, Voldman J. 2013. Matrix remodeling maintains ESC self-renewal by activating Stat3. *Stem Cells* 31:1097–106
33. Kloxin AM, Kasko AM, Salinas CN, Anseth KS. 2009. Photodegradable hydrogels for dynamic tuning of physical and chemical properties. *Science* 324:59–63
34. Tan CP, Seo BR, Brooks DJ, Chandler EM, Craighead HG, Fischbach C. 2009. Parylene peel-off arrays to probe the role of cell–cell interactions in tumour angiogenesis. *Integr. Biol.* 1:587–94
35. Li CY, Wood DK, Hsu CM, Bhatia SN. 2011. DNA-templated assembly of droplet-derived PEG microtissues. *Lab Chip* 11:2967–75
36. Robertus J, Browne WR, Feringa BL. 2010. Dynamic control over cell adhesive properties using molecular-based surface engineering strategies. *Chem. Soc. Rev.* 39:354–78
37. Wu LY, Di Carlo D, Lee LP. 2008. Microfluidic self-assembly of tumor spheroids for anticancer drug discovery. *Biomed. Microdevices* 10:197–202
38. Yarmush ML, King KR. 2009. Living-cell microarrays. *Annu. Rev. Biomed. Eng.* 11:235–57
39. Zervantonakis IK, Kothapalli CR, Chung S, Sudo R, Kamm RD. 2011. Microfluidic devices for studying heterotypic cell-cell interactions and tissue specimen cultures under controlled microenvironments. *Biomicrofluidics* 5:14
40. Lee GH, Lee JS, Wang X, Hoon Lee S. 2016. Bottom-up engineering of well-defined 3D microtissues using microplatforms and biomedical applications. *Adv. Healthc. Mater.* 5:56–74
41. Albrecht DR, Underhill GH, Wassermann TB, Sah RL, Bhatia SN. 2006. Probing the role of multicellular organization in three-dimensional microenvironments. *Nat. Methods* 3:369–75
42. Gu L, Mooney DJ. 2016. Biomaterials and emerging anticancer therapeutics: engineering the microenvironment. *Nat. Rev. Cancer* 16:56–66
43. Murphy SV, Atala A. 2014. 3D bioprinting of tissues and organs. *Nat. Biotech.* 32:773–85
44. Woolfson DN, Mahmoud ZN. 2010. More than just bare scaffolds: towards multi-component and decorated fibrous biomaterials. *Chem. Soc. Rev.* 39:3464–79
45. Yin X, Mead BE, Safaee H, Langer R, Karp JM, Levy O. 2016. Engineering stem cell organoids. *Cell Stem Cell* 18:25–38
46. Hwang YS, Chung BG, Ortmann D, Hattori N, Moeller HC, Khademhosseini A. 2009. Microwell-mediated control of embryoid body size regulates embryonic stem cell fate via differential expression of WNT5a and WNT11. *PNAS* 106:16978–83
47. Lee LH, Peerani R, Ungrin M, Joshi C, Kumacheva E, Zandstra PW. 2009. Micropatterning of human embryonic stem cells dissects the mesoderm and endoderm lineages. *Stem Cell Res.* 2:155–62
48. Peerani R, Zandstra PW. 2010. Enabling stem cell therapies through synthetic stem cell-niche engineering. *J. Clin. Invest.* 120:60–70
49. Sung KE, Yang N, Pehlke C, Keely PJ, Eliceiri KW, et al. 2011. Transition to invasion in breast cancer: A microfluidic in vitro model enables examination of spatial and temporal effects. *Integr. Biol.* 3:439–50
50. Chen D, Du WB, Liu Y, Liu WS, Kuznetsov A, et al. 2008. The chemistrode: a droplet-based microfluidic device for stimulation and recording with high temporal, spatial, and chemical resolution. *PNAS* 105:16843–48
51. Kaigala GV, Lovchik RD, Drechsler U, Delamarche E. 2011. A vertical microfluidic probe. *Langmuir* 27:5686–93
52. Saha-Shah A, Green CM, Abraham DH, Baker LA. 2016. Segmented flow sampling with push–pull theta pipettes. *Analyst* 141:1958–65
53. Ross AE, Belanger MC, Woodroof JF, Pompano RR. 2017. Spatially resolved microfluidic stimulation of lymphoid tissue *ex vivo*. *Analyst* 142:649–59

54. Chang TC, Mikheev AM, Huynh W, Monnat RJ, Rostomily RC, Folch A. 2014. Parallel microfluidic chemosensitivity testing on individual slice cultures. *Lab Chip* 14:4540–51
55. Huang Y, Williams JC, Johnson SM. 2012. Brain slice on a chip: opportunities and challenges of applying microfluidic technology to intact tissues. *Lab Chip* 12:2103–17
56. Mohammed JS, Caicedo HH, Fall CP, Eddington DT. 2008. Microfluidic add-on for standard electrophysiology chambers. *Lab Chip* 8:1048–55
57. Queval A, Ghattamaneni NR, Perrault CM, Gill R, Mirzaei M, et al. 2010. Chamber and microfluidic probe for microperfusion of organotypic brain slices. *Lab Chip* 10:326–34
58. Tang YT, Kim J, Lopez-Valdes HE, Brennan KC, Ju YS. 2011. Development and characterization of a microfluidic chamber incorporating fluid ports with active suction for localized chemical stimulation of brain slices. *Lab Chip* 11:2247–54
59. Yi Y, Park J, Lim J, Lee CJ, Lee S-H. 2015. Central nervous system and its disease models on a chip. *Trends Biotechnol.* 33:762–76
60. Campenot RB. 1977. Local control of neurite development by nerve growth factor. *PNAS* 74:4516–19
61. Tang YT, Mendez JM, Theriot JJ, Sawant PM, Lopez-Valdes HE, et al. 2014. Minimum conditions for the induction of cortical spreading depression in brain slices. *J. Neurophysiol.* 112:2572–79
62. Good MC, Zalatan JG, Lim WA. 2011. Scaffold proteins: hubs for controlling the flow of cellular information. *Science* 332:680–86
63. Chen C-C, Wang L, Plikus MV, Jiang TX, Murray PJ, et al. 2015. Organ-level quorum sensing directs regeneration in hair stem cell populations. *Cell* 161:277–90
64. Kastrup CJ, Boedicker JQ, Pomerantsev AP, Moayeri M, Bian Y, et al. 2008. Spatial localization of bacteria controls coagulation of human blood by 'quorum acting.' *Nat. Chem. Biol.* 4:742–50
65. Hui EE, Bhatia SN. 2007. Micromechanical control of cell–cell interactions. *PNAS* 104:5722–26
66. Rosenthal A, Macdonald A, Voldman J. 2007. Cell patterning chip for controlling the stem cell microenvironment. *Biomaterials* 28:3208–16
67. Lee WH, Ngernsutivorakul T, Mabrouk OS, Wong J-MT, Dugan CE, et al. 2016. Microfabrication and in vivo performance of a microdialysis probe with embedded membrane. *Anal. Chem.* 88:1230–37
68. Slaney TR, Nie J, Hershey ND, Thwar PK, Linderman J, et al. 2011. Push-pull perfusion sampling with segmented flow for high temporal and spatial resolution in vivo chemical monitoring. *Anal. Chem.* 83:5207–13
69. Clement AM, Nguyen MD, Roberts EA, Garcia ML, Boillee S, et al. 2003. Wild-type nonneuronal cells extend survival of SOD1 mutant motor neurons in ALS mice. *Science* 302:113–17
70. Kastrup CJ, Nahrendorf M, Figueiredo JL, Lee H, Kambhampati S, et al. 2012. Painting blood vessels and atherosclerotic plaques with an adhesive drug depot. *PNAS* 109:21444–49
71. Kolambkar YM, Dupont KM, Boerckel JD, Huebsch N, Mooney DJ, et al. 2011. An alginate-based hybrid system for growth factor delivery in the functional repair of large bone defects. *Biomaterials* 32:65–74
72. Mitragotri S, Burke PA, Langer R. 2014. Overcoming the challenges in administering biopharmaceuticals: formulation and delivery strategies. *Nat. Rev. Drug Discov.* 13:655–72
73. Patterson J, Martino MM, Hubbell JA. 2010. Biomimetic materials in tissue engineering. *Mater. Today* 13:14–22
74. Schoellhammer CM, Schroeder A, Maa R, Lauwers GY, Swiston A, et al. 2015. Ultrasound-mediated gastrointestinal drug delivery. *Sci. Transl. Med.* 7:310ra168
75. Borselli C, Storrie H, Benesch-Lee F, Shvartsman D, Cezar C, et al. 2010. Functional muscle regeneration with combined delivery of angiogenesis and myogenesis factors. *PNAS* 107:3287–92
76. Furie B, Furie BC. 2012. Formation of the clot. *Thromb. Res.* 130(Suppl. 1):S44–46
77. Tischer D, Weiner OD. 2014. Illuminating cell signalling with optogenetic tools. *Nat. Rev. Mol. Cell Biol.* 15:551–58
78. Peinado H, Lavotshkin S, Lyden D. 2011. The secreted factors responsible for pre-metastatic niche formation: old sayings and new thoughts. *Semin. Cancer Biol.* 21:139–46
79. Dargan SL, Schwaller B, Parker I. 2004. Spatiotemporal patterning of $IP_3$-mediated $Ca^{2+}$ signals in *Xenopus* oocytes by $Ca^{2+}$-binding proteins. *J. Physiol.* 556:447–61

80. Ivanciu L, Stalker TJ. 2015. Spatiotemporal regulation of coagulation and platelet activation during the hemostatic response in vivo. *J. Thromb. Haemost.* 13:1949–59
81. Griffith LG, Swartz MA. 2006. Capturing complex 3D tissue physiology in vitro. *Nat. Rev. Mol. Cell Biol.* 7:211–24
82. Proudfoot AEI. 2006. The biological relevance of chemokine–proteoglycan interactions. *Biochem. Soc. Trans.* 34:422–26
83. Swartz MA, Fleury ME. 2007. Interstitial flow and its effects in soft tissues. *Annu. Rev. Biomed. Eng.* 9:229–56
84. Magzoub M, Jin S, Verkman AS. 2008. Enhanced macromolecule diffusion deep in tumors after enzymatic digestion of extracellular matrix collagen and its associated proteoglycan decorin. *FASEB J.* 22:276–84
85. Kim J, Cao L, Shvartsman D, Silva EA, Mooney DJ. 2011. Targeted delivery of nanoparticles to ischemic muscle for imaging and therapeutic angiogenesis. *Nano Lett.* 11:694–700
86. Dityatev A, Seidenbecher CI, Schachner M. 2010. Compartmentalization from the outside: the extracellular matrix and functional microdomains in the brain. *Trends Neurosci.* 33:503–12
87. Sykova E, Nicholson C. 2008. Diffusion in brain extracellular space. *Physiol. Rev.* 88:1277–340
88. Chauhan VP, Lanning RM, Diop-Frimpong B, Mok W, Brown EB, et al. 2009. Multiscale measurements distinguish cellular and interstitial hindrances to diffusion in vivo. *Biophys. J.* 97:330–36
89. Netti PA, Berk DA, Swartz MA, Grodzinsky AJ, Jain RK. 2000. Role of extracellular matrix assembly in interstitial transport in solid tumors. *Cancer Res.* 60:2497–503
90. Khanvilkar K, Donovan MD, Flanagan DR. 2001. Drug transfer through mucus. *Adv. Drug Deliv. Rev.* 48:173–93
91. Stewart PS. 2003. Diffusion in biofilms. *J. Bacteriol.* 185:1485–91
92. Ward KW. 2008. A review of the foreign-body response to subcutaneously-implanted devices: The role of macrophages and cytokines in biofouling and fibrosis. *J. Diabetes Sci. Technol.* 2:768–77
93. Sachlos E, Auguste DT. 2008. Embryoid body morphology influences diffusive transport of inductive biochemicals: a strategy for stem cell differentiation. *Biomaterials* 29:4471–80
94. Hynes RO. 2009. The extracellular matrix: not just pretty fibrils. *Science* 326:1216–19
95. Francavilla C, Papetti M, Rigbolt KT, Pedersen AK, Sigurdsson JO, et al. 2016. Multilayered proteomics reveals molecular switches dictating ligand-dependent EGFR trafficking. *Nat. Struct. Mol. Biol.* 23:608–18
96. Dona E, Barry JD, Valentin G, Quirin C, Khmelinskii A, et al. 2013. Directional tissue migration through a self-generated chemokine gradient. *Nature* 503:285–89
97. Dai E, Liu LY, Wang H, McIvor D, Sun YM, et al. 2010. Inhibition of chemokine-glycosaminoglycan interactions in donor tissue reduces mouse allograft vasculopathy and transplant rejection. *PLOS ONE* 5:e10510
98. Proudfoot AEI, Handel TM, Johnson Z, Lau EK, LiWang P, et al. 2003. Glycosaminoglycan binding and oligomerization are essential for the *in vivo* activity of certain chemokines. *PNAS* 100:1885–90
99. Brown JM, Xia J, Zhuang B, Cho KS, Rogers CJ, et al. 2012. A sulfated carbohydrate epitope inhibits axon regeneration after injury. *PNAS* 109:4768–73
100. Custodio CA, Reis RL, Mano JF. 2014. Engineering biomolecular microenvironments for cell instructive biomaterials. *Adv. Healthc. Mater.* 3:797–810
101. Martino MM, Tortelli F, Mochizuki M, Traub S, Ben-David D, et al. 2011. Engineering the growth factor microenvironment with fibronectin domains to promote wound and bone tissue healing. *Sci. Transl. Med.* 3:100ra89
102. Das RK, Zouani OF. 2014. A review of the effects of the cell environment physicochemical nanoarchitecture on stem cell commitment. *Biomaterials* 35:5278–93
103. Wong AP, Perez-Castillejos R, Christopher Love J, Whitesides GM. 2008. Partitioning microfluidic channels with hydrogel to construct tunable 3-D cellular microenvironments. *Biomaterials* 29:1853–61
104. Tien J, Nelson CM. 2014. Microstructured extracellular matrices in tissue engineering and development: an update. *Ann. Biomed. Eng.* 42:1413–23
105. Chen S, Lee LP. 2010. Non-invasive microfluidic gap junction assay. *Integr. Biol.* 2:130–38

106. Chan V, Novakowski SK, Law S, Klein-Bosgoed C, Kastrup CJ. 2015. Controlled transcription of exogenous mRNA in platelets using protocells. *Angew. Chem. Int. Ed. Engl.* 54:13590–93
107. Lizana L, Bauer B, Orwar O. 2008. Controlling the rates of biochemical reactions and signaling networks by shape and volume changes. *PNAS* 105:4099–104
108. Gorris HH, Walt DR. 2010. Analytical chemistry on the femtoliter scale. *Angew. Chem. Int. Ed. Engl.* 49:3880–95
109. Vincent ME, Liu WS, Haney EB, Ismagilov RF. 2010. Microfluidic stochastic confinement enhances analysis of rare cells by isolating cells and creating high density environments for control of diffusible signals. *Chem. Soc. Rev.* 39:974–84
110. Weitz M, Mückl A, Kapsner K, Berg R, Meyer A, Simmel FC. 2014. Communication and computation by bacteria compartmentalized within microemulsion droplets. *J. Am. Chem. Soc.* 136:72–75
111. Boedicker JQ, Vincent ME, Ismagilov RF. 2009. Microfluidic confinement of single cells of bacteria in small volumes initiates high-density behavior of quorum sensing and growth and reveals its variability. *Angew. Chem. Int. Ed. Engl.* 48:5908–11
112. Connell JL, Wessel AK, Parsek MR, Ellington AD, Whiteley M, Shear JB. 2010. Probing prokaryotic social behaviors with bacterial "lobster traps." *mBio* 1:e00202-10
113. Carnes EC, Lopez DM, Donegan NP, Cheung A, Gresham H, et al. 2010. Confinement-induced quorum sensing of individual *Staphylococcus aureus* bacteria. *Nat. Chem. Biol.* 6:41–45
114. Hagen SJ, Son M, Weiss JT, Young JH. 2010. Bacterium in a box: sensing of quorum and environment by the LuxI/LuxR gene regulatory circuit. *J. Biol. Phys.* 36:317–27
115. Luthuli BB, Purdy GE, Balagadde FK. 2015. Confinement-induced drug-tolerance in mycobacteria mediated by an efflux mechanism. *PLOS ONE* 10:e0136231
116. Yu HM, Meyvantsson I, Shkel IA, Beebe DJ. 2005. Diffusion dependent cell behavior in microenvironments. *Lab Chip* 5:1089–95
117. Tschumperlin DJ, Dai G, Maly IV, Kikuchi T, Laiho LH, et al. 2004. Mechanotransduction through growth-factor shedding into the extracellular space. *Nature* 429:83–86
118. Sato T, van Es JH, Snippert HJ, Stange DE, Vries RG, et al. 2011. Paneth cells constitute the niche for Lgr5 stem cells in intestinal crypts. *Nature* 469:415–18
119. Magliozzi R, Howell O, Vora A, Serafini B, Nicholas R, et al. 2007. Meningeal B-cell follicles in secondary progressive multiple sclerosis associate with early onset of disease and severe cortical pathology. *Brain* 130:1089–104
120. Park S, Wolanin PM, Yuzbashyan EA, Silberzan P, Stock JB, Austin RH. 2003. Motion to form a quorum. *Science* 301:188
121. Ribbe J, Maier B. 2016. Density-dependent differentiation of bacteria in spatially structured open systems. *Biophys. J.* 110:1648–60
122. Shen F, Pompano RR, Kastrup CJ, Ismagilov RF. 2009. Confinement regulates complex biochemical networks: initiation of blood clotting by "diffusion acting." *Biophys. J.* 97:2137–45
123. Hathcock JJ. 2006. Flow effects on coagulation and thrombosis. *Arterioscler. Thromb. Vasc. Biol.* 26:1729–37
124. Wyffels K, Kaanders J, Rijken P, Bussink J, van den Hoogen FJA, et al. 2000. Vascular architecture and hypoxic profiles in human head and neck squamous cell carcinomas. *Br. J. Cancer* 83:674–83
125. Kuo JS, Chiu DT. 2011. Controlling mass transport in microfluidic devices. *Annu. Rev. Anal. Chem.* 4:275–96
126. Okorie UM, Denney WS, Chatterjee MS, Neeves KB, Diamond SL. 2008. Determination of surface tissue factor thresholds that trigger coagulation at venous and arterial shear rates: amplification of 100 fM circulating tissue factor requires flow. *Blood* 111:3507–13
127. Shen F, Kastrup CJ, Liu Y, Ismagilov RF. 2008. Threshold response of initiation of blood coagulation by tissue factor in patterned microfluidic capillaries is controlled by shear rate. *Arterioscler. Thromb. Vasc. Biol.* 28:2035–41
128. Alonzo LF, Moya ML, Shirure VS, George SC. 2015. Microfluidic device to control interstitial flow-mediated homotypic and heterotypic cellular communication. *Lab Chip* 15:3521–29
129. Choi NW, Cabodi M, Held B, Gleghorn JP, Bonassar LJ, Stroock AD. 2007. Microfluidic scaffolds for tissue engineering. *Nat. Mater.* 6:908–15

130. Bonvin C, Overney J, Shieh AC, Dixon JB, Swartz MA. 2010. A multichamber fluidic device for 3D cultures under interstitial flow with live imaging: development, characterization, and applications. *Biotechnol. Bioeng.* 105:982–91
131. Baylis JR, Yeon JH, Thomson MH, Kazerooni A, Wang X, et al. 2015. Self-propelled particles that transport cargo through flowing blood and halt hemorrhage. *Sci. Adv.* 1:e1500379
132. Gao W, Dong R, Thamphiwatana S, Li J, Gao W, et al. 2015. Artificial micromotors in the mouse's stomach: a step toward in vivo use of synthetic motors. *ACS Nano* 9:117–23
133. Srivastava SK, Medina-Sanchez M, Koch B, Schmidt OG. 2016. Medibots: dual-action biogenic microdaggers for single-cell surgery and drug release. *Adv. Mater.* 28:832–37
134. Schmitz ML, Weber A, Roxlau T, Gaestel M, Kracht M. 2011. Signal integration, crosstalk mechanisms and networks in the function of inflammatory cytokines. *Biochim. Biophys. Acta Mol. Cell Res.* 1813:2165–75
135. Vaday GG, Lider O. 2000. Extracellular matrix moieties, cytokines, and enzymes: dynamic effects on immune cell behavior and inflammation. *J. Leukoc. Biol.* 67:149–59
136. Lassmann H. 2011. Review: the architecture of inflammatory demyelinating lesions: implications for studies on pathogenesis. *Neuropathol. Appl. Neurobiol.* 37:698–710
137. Gao HM, Hong JS. 2008. Why neurodegenerative diseases are progressive: Uncontrolled inflammation drives disease progression. *Trends Immunol.* 29:357–65
138. Akassoglou K, Adams RA, Bauer J, Mercado P, Tseveleki V, et al. 2004. Fibrin depletion decreases inflammation and delays the onset of demyelination in a tumor necrosis factor transgenic mouse model for multiple sclerosis. *PNAS* 101:6698–703
139. Marik C, Felts PA, Bauer J, Lassmann H, Smith KJ. 2007. Lesion genesis in a subset of patients with multiple sclerosis: a role for innate immunity? *Brain* 130:2800–15
140. van der Valk P, Amor S. 2009. Preactive lesions in multiple sclerosis. *Curr. Opin. Neurol.* 22:207–13
141. Bhatia SN, Ingber DE. 2014. Microfluidic organs-on-chips. *Nat. Biotech.* 32:760–72
142. Choi CK, Breckenridge MT, Chen CS. 2010. Engineered materials and the cellular microenvironment: a strengthening interface between cell biology and bioengineering. *Trends Cell Biol.* 20:705–14
143. Wang M, Hershey ND, Mabrouk OS, Kennedy RT. 2011. Collection, storage, and electrophoretic analysis of nanoliter microdialysis samples collected from awake animals in vivo. *Anal. Bioanal. Chem.* 400:2013–23
144. Cepeda DE, Hains L, Li D, Bull J, Lentz SI, Kennedy RT. 2015. Experimental evaluation and computational modeling of tissue damage from low-flow push–pull perfusion sampling in vivo. *J. Neurosci. Methods* 242:97–105
145. Bucher ES, Wightman RM. 2015. Electrochemical analysis of neurotransmitters. *Annu. Rev. Anal. Chem.* 8:239–61
146. Andersson U, Tracey KJ. 2012. Neural reflexes in inflammation and immunity. *J. Exp. Med.* 209:1057–68
147. Germain RN, Robey EA, Cahalan MD. 2012. A decade of imaging cellular motility and interaction dynamics in the immune system. *Science* 336:1676–81
148. Reynolds F, Kelly KA. 2011. Techniques for molecular imaging probe design. *Mol. Imaging* 10:407–19
149. Porterfield WB, Prescher JA. 2015. Tools for visualizing cell–cell 'interactomes.' *Curr. Opin. Chem. Biol.* 24:121–30
150. Shapiro MG, Goodwill PW, Neogy A, Yin M, Foster FS, et al. 2014. Biogenic gas nanostructures as ultrasonic molecular reporters. *Nat. Nanotechnol.* 9:311–16
151. Shapiro MG, Ramirez RM, Sperling LJ, Sun G, Sun J, et al. 2014. Genetically encoded reporters for hyperpolarized xenon magnetic resonance imaging. *Nat. Chem.* 6:629–34
152. Crosetto N, Bienko M, van Oudenaarden A. 2015. Spatially resolved transcriptomics and beyond. *Nat. Rev. Genet.* 16:57–66
153. Miesenbock G. 2009. The optogenetic catechism. *Science* 326:395–99
154. Ryu KA, Stutts L, Tom JK, Mancini RJ, Esser-Kahn AP. 2014. Stimulation of innate immune cells by light-activated TLR7/8 agonists. *J. Am. Chem. Soc.* 136:10823–25
155. Bansal A, Zhang Y. 2014. Photocontrolled nanoparticle delivery systems for biomedical applications. *Acc. Chem. Res.* 47:3052–60

156. Aryal M, Arvanitis CD, Alexander PM, McDannold N. 2014. Ultrasound-mediated blood–brain barrier disruption for targeted drug delivery in the central nervous system. *Adv. Drug Deliv. Rev.* 72:94–109
157. Jeong J-W, McCall JG, Shin G, Zhang Y, Al-Hasani R, et al. 2015. Wireless optofluidic systems for programmable in vivo pharmacology and optogenetics. *Cell* 162:662–74
158. Purwada A, Jaiswal MK, Ahn H, Nojima T, Kitamura D, et al. 2015. Ex vivo engineered immune organoids for controlled germinal center reactions. *Biomaterials* 63:24–34
159. Singh A, Peppas NA. 2014. Hydrogels and scaffolds for immunomodulation. *Adv. Mater.* 26:6530–41
160. Farra R, Sheppard NF Jr., McCabe L, Neer RM, Anderson JM, et al. 2012. First-in-human testing of a wirelessly controlled drug delivery microchip. *Sci. Transl. Med.* 4:122ra21
161. Chang A, Smith MC, Yin XH, Fox RJ, Staugaitis SM, Trapp BD. 2008. Neurogenesis in the chronic lesions of multiple sclerosis. *Brain* 131:2366–75

**TABLE OF CONTENTS FOR VOLUME 1:**

Annual Review of Biochemistry
Volume 86, 2017

# Contents

**Errata**

An online log of corrections to *Annual Review of Biochemistry* articles may be found at http://www.annualreviews.org/errata/biochem